NIH Public Access
Author Manuscript
Bone. Author manuscript; available in PMC 2012 December 1.

Published in final edited form as:
Bone. 2011 December ; 49(6): 1279–1289. doi:10.1016/j.bone.2011.09.042.

Mechanical property and tissue mineral density differences among severely suppressed bone turnover (SSBT) patients, osteoporotic patients, and normal subjects

Crystal Tjhia[a,b], **Clarita V. Odvina**[c], **D. Sudhaker Rao**[d], **Susan M. Stover**[e], **Xiang Wang**[a], and **David Fyhrie**[a,b]

[a]Lawrence J. Ellison Musculoskeletal Research Center, University of California Davis Medical Center, Sacramento, CA, USA

[b]Department of Biomedical Engineering, University of California, Davis, CA, USA

[c]Charles and Jane Pak Center for Mineral Metabolism and Clinical Research, University of Texas Southwestern Medical Center, Dallas, TX, USA

[d] Bone and Mineral Research Laboratory, Henry Ford Hospital, Detroit, MI, USA

[e]Department of Anatomy, Physiology and Cell Biology, School of Veterinary Medicine, University of California, Davis, CA, USA

Abstract

Pathogenesis of atypical fractures in patients on long term bisphosphonate therapy is poorly understood, and the type, the manner in which they occur and the fracture sites are quite different from the usual osteoporotic fractures. We hypothesized that the tissue-level mechanical properties and mean degree of mineralization of the iliac bone would differ among 1) patients with atypical fractures and severely suppressed bone turnover (SSBT) associated with long-term bisphosphonate therapy, 2) age-matched, treatment-naïve osteoporotic patients with vertebral fracture, 3) age-matched normals and 4) young normals. Large differences in tissue-level mechanical properties and/or mineralization among these groups could help explain the underlying mechanism(s) for the occurrence of typical osteoporotic and the atypical femoral shaft fractures. Elastic modulus, contact hardness, plastic deformation resistance, and tissue mineral densities of cortical and trabecular bone regions of 55 iliac bone biopsies—12 SSBT patients (SSBT; aged 49–77), 11 age-matched untreated osteoporotic patients with vertebral fracture (Osteoporotic), 12 age-matched subjects without bone fracture (Age-Matched Normal), and 20 younger subjects without bone fracture (Young Normal)—were measured using nanoindentation and quantitative backscattered electron microscopy. For cortical bone nanoindentation properties, only plastic deformation resistance was different among the groups ($p<0.05$), with greater resistance to plastic deformation in the SSBT group compared to all other groups. For trabecular bone, all nanoindentation properties and mineral density of the trabecular bone were different among the groups ($p<0.05$). The SSBT group had greater plastic deformation resistance and harder trabecular

© Published by Elsevier Inc.

Please address all correspondence to: Crystal Tjhia Lawrence J. Ellison Musculoskeletal Research Center University of California Davis Medical Center Research Building 1, Room 2000 4635 Second Avenue Sacramento, CA 95817 Phone: (916) 734-5745 Fax: (916) 734-5750 ctjhia@ucdavis.edu.

Publisher's Disclaimer: This is a PDF file of an unedited manuscript that has been accepted for publication. As a service to our customers we are providing this early version of the manuscript. The manuscript will undergo copyediting, typesetting, and review of the resulting proof before it is published in its final citable form. Please note that during the production process errors may be discovered which could affect the content, and all legal disclaimers that apply to the journal pertain.

Disclosures: None

NIH-PA Author Manuscript
NIH-PA Author Manuscript
NIH-PA Author Manuscript

NIH-PA Author Manuscript

NIH-PA Author Manuscript

NIH-PA Author Manuscript

bone compared to the other three groups, stiffer bone compared to the Osteoporotic and Young Normal groups, and a trend of higher mineral density compared to the Age-Matched Normal and Osteoporotic groups. Lower heterogeneity of modulus and contact hardness for cortical bone of the SSBT and trabecular bone of the Osteoporotic fracture groups, respectively, compared to the non-fractured groups, may contribute to fracture susceptibility due to lowered ability to prevent crack propagation. We tentatively conclude that, in addition to extremely low bone formation rate, atypical fractures in SSBT and/or long-term bisphosphonate treatment may be associated with greater mean plastic deformation resistance properties and less heterogeneous elastic properties of the bone.

Keywords

Bisphosphonate; Atypical fracture; Severely suppressed bone turnover; Nanoindentation; Mechanical properties; Mineral density

Introduction

Fractures occur among the elderly at a higher rate compared to younger healthy individuals. The causes of fracture are many, but the general observation is that the majority of fracture patients have normal hard tissue, just not enough of it [1]. In the absence of metabolic bone disease, therefore, treatment of osteoporosis has concentrated on prevention of bone loss. Recently, however, there have been reports of patients treated for osteoporosis who sustained atypical fractures during treatment with bisphosphonates [2–7]. Atypical fractures occur in bone regions that are composed of mostly cortical bone such as the femoral shaft, in contrast to typical osteoporotic fractures that occur in the spine, hip, and wrist, regions that contain mostly trabecular bone. The unusual locations of atypical fractures indicate that low bone mass may not be the reason for these fractures, but the exact cause of these fractures is not well understood.

It is not known whether atypical fracture patients have hard tissue properties that increase their susceptibility to atraumatic nonvertebral fractures. Specific features of atypical fractures, as defined by the American Society for Bone and Mineral Research (ASBMR) task force [8], indicate the possibility of changed material properties of the bone. Observations of cortical thickening and periosteal stress reaction in radiographs of atypical fracture sites indicate a stress fracture-like behavior, which may be associated with an accumulation of microdamage or changed material properties [9]. Another major feature of the atypical femoral fracture is the transverse or short oblique configuration, characteristic of failure of brittle material [5, 6], which suggests that the tissue-level properties may be associated with increased likelihood of fracture occurrence. Studies of the effects of bisphosphonate-induced suppression of bone turnover in dogs provide evidence of decreased toughness, or energy absorption to failure, and increased mineralization density along with increased microdamage, compared to untreated controls [10–13]. However data of direct measurements of material properties of bone tissue from atypical fracture patients are limited.

In this study, we measured the tissue level mechanical properties and mineral densities of a subset of patients on long-term bisphosphonate treatment who had atypical fractures and severely suppressed bone turnover (SSBT). Suppressed bone turnover, measured by histomorphometry of biopsy tissue, has been observed in some case studies of patients with atypical fractures [8]. Our SSBT patient group was collected prior to the convening of the ASBMR task force, and was part of the original observations of patients with atypical fractures [14, 15]. It is unknown whether patients who suffer from atypical fractures and

NIH-PA Author Manuscript

NIH-PA Author Manuscript

NIH-PA Author Manuscript

SSBT or low bone formation rates had low bone turnover before bisphosphonate treatment. As a result, the data presented here could tell us whether *this group* of patients with atypical fracture and low bone formation rate has abnormal hard tissue properties. However, not all patients with atypical fracture have SSBT, and not all patients with low bone turnover have atypical fractures.

The patients with atypical fracture included in the present study were from the 22 patients previously reported [14, 15]. Nine patients each had at least one atraumatic nonvertebral fracture associated with delayed or absent fracture healing [15]. All patients were prescribed alendronate for a minimum of 3 years for the treatment of osteoporosis or osteopenia. Iliac bone histomorphometric revealed SSBT, characterized by lack of double tetracycline labels and little or no osteoblast surface. Five of the 9 patients were taking estrogen or glucocorticoids concomitantly with alendronate. A second report identified 13 additional patients that each had at least one atraumatic long bone mid-shaft fracture while on alendronate or risedronate treatment [14]. Histomorphometric analysis of the trans iliac bone biopsies obtained from 6 of these patients also showed low bone turnover.

One potential mechanism for the pathogenesis of atypical fracture in SSBT patients is a failure to repair microdamage [10–13, 16, 17]. An alternative explanation is that patients with atypical fractures have abnormally weak hard tissue properties that result in fractures, despite therapy. The objectives of the experiments reported here were to 1) measure the hard tissue properties in young and age-matched normals, untreated osteoporotic patients with vertebral fractures and long-term bisphosphonate treated SSBT patients and 2) determine whether the observed mechanical properties support a hypothesis that patients with SSBT have abnormal hard tissue material properties. Potential differences in mechanical properties and mineral composition are not restricted to those caused by drug treatment, but also include any pre-existing differences in the bone quality of the SSBT patients that could contribute to their unusual fractures.

Methods

Samples and specimen preparation

Trans iliac core biopsy specimens (55 total) from SSBT patients, osteoporotic patients with vertebral fracture, and non-fracture subjects were obtained from biopsy collections at Henry Ford Hospital (HFH; Detroit, MI) and Southwestern Medical Center (SMC; Dallas, TX) (Table 1). The 12 SSBT biopsies were a subset of the 22 patients we originally used to define SSBT [14, 15]. All biopsies, but one, were from women, and the detailed bone histomorphometric data have been reported [14, 15]. Although the vast majority had SSBT, a few patients exhibited occasional single labels, from which we imputed bone formation rate (BFR) by assuming a mineral apposition rate of 0.3 micrometers per day as we previously reported [18]. SSBT biopsies were compared to young normal (YgN) and age-matched normal subjects (AMN), as well as osteoporotic patients with vertebral fracture (OP). The young subjects had a lower mean age than the ages of all other groups, which were not different from each other. All biopsies from normal subjects and osteoporotic patients were from a library of biopsies collected at HFH between 1980 and 1992 and were performed by a single operator (DSR). The SSBT biopsies from both the HFH and the SMC were collected between 2001 and 2007. Trabecular BFR per bone surface was measured for all 55 biopsies using standard methods ([15, 19]; Table 1). The BFRs measured at trabecular sites were different among groups ($p=0.004$), and the BFR in the SSBT group was significantly lower than the other 3 groups, which were not statistically different from each other.

NIH-PA Author Manuscript

NIH-PA Author Manuscript

NIH-PA Author Manuscript

Biopsies in both laboratories were pre-stained for 72 hours in Villanueva bone stain, and then dehydrated in increasing concentrations of alcohol. Samples were embedded in poly(methyl methacrylate) (PMMA) blocks for detailed histomorphometric study, following the laboratory-specific protocols. The samples at the SMC were embedded in 85% methyl methacrylate, with 15% dibutyl phthalate added as a plastic softener. Perkadox 16 (AzkoNobel, Amsterdam, the Netherlands) was the polymerization initiator. The HFH biopsies were prepared in 100% methyl methacrylate with benzoyl peroxide to initiate polymerization.

Both cortical and trabecular bone regions were exposed on one block face of each biopsy. As is standard, the biopsies were oriented so that the block face was cut along the axis of the cylindrical biopsy.

The bottom of each biopsy block was milled flat such that the top and bottom faces were parallel. The face with the exposed bone was polished to a mirror finish with successively finer grits of carborundum paper and alumina polishing powders (Buehler Ltd., Lake Bluff, Illinois). The smallest alumina particle size was 0.05 μm.

Nanoindentation

Mechanical property measurements were performed using a Nanoindenter XP instrument (Agilent Technologies Inc., Oak Ridge, TN). Nanoindentation is a form of instrumented indentation, in which load and displacement are monitored at high resolution (50 nN and 0.01 nm, respectively) as the tip of a probe is pressed into the surface of a polished sample. A Berkovich pyramidal diamond tip was used to probe for mechanical properties (tip radius <20 nm). Elastic modulus (E) and contact hardness (H_c) were calculated using the Oliver-Pharr method [20]. In this method, elastic modulus is a function of the unloading stiffness of the force-displacement curve, under the assumption that the unloading is elastic. Contact hardness is calculated as the maximum load divided by the projected area of the indenter tip (6.18 μm^2) at maximum load. Since elastic and plastic deformations contribute to the deformation at maximum load, contact hardness is derived from both the elastic and plastic properties of the material. To characterize the plastic behavior, resistance to plastic deformation (H) was also calculated using an expression derived by Sakai [21], which has been applied to nanoindentation data of mineralized tissues [22]. Plastic deformation resistance is a function of the elastic modulus and contact hardness from the indentation test and 2 constant terms associated with the geometry of the indenter tip. The underlying assumptions for this calculation are that the material behavior can be characterized as elastic-plastic and that the elastic and plastic deformations occur in series.

A typical load-displacement curve is shown in Fig. 1. For each test, the indenter approached the surface at10 nm/s. Once the surface was detected, the tip advanced at a target strain rate of 0.05 s^{-1} to maximum depth of 500 nm in order to minimize the effect of surface roughness [23] and accurately measure elastic modulus [24]. Strain rate is defined as the instantaneous rate of displacement of the indenter tip divided by the displacement at that instant in time [25]. The indenter was held at the maximum load for ten seconds, then unloaded to 10% of the maximum load for a second hold period of 100 seconds to account for thermal drift. Fluctuations in displacement measurements during this hold period were attributed to thermal expansion and contraction of the sample and indenter equipment. These values were recorded and the calculated drift rate was used to correct the displacement measurements taken during the duration of the indentation test, assuming a constant drift rate throughout the indentation test (TestWorks software, Agilent Technologies, Inc., Oak Ridge, TN). Poisson's ratio of bone was assumed to be 0.30 [26]. Poisson's ratio of PMMA was assumed to be 0.35 as reported in the literature [27].

NIH-PA Author Manuscript

NIH-PA Author Manuscript

NIH-PA Author Manuscript

Indents were positioned at cortical and trabecular bone regions using a built-in 10× light objective. For each biopsy, three to five trabeculae, irrespective of orientation, were selected at random for indentation across the width of the bony region (Fig. 2) for a total of approximately 30 indents. For each trabecular region, a one-dimensional array of indents was set up such that the first and last indents were positioned outside of the bone area in the surrounding PMMA. This method ensured that the entire width of each trabecula was sampled. Previous work demonstrated that deep and shallow trabecular tissue can have different mineralization properties [28]. Thus we aimed to capture the range in properties across the thickness of a trabecula and no effort was made to position indents within similar microstructural features. Similarly, two linear arrays across the width of the cortex were indented for a total of 30 cortical bone indentations. Indentations were also made in the PMMA embedding material at locations away from the bone, since the properties of the PMMA were found to vary among specimens. Distance between the indentations was 20 micrometers or greater such that the volumes of indentation from neighboring tests did not interact [29].

Some mechanical property data from the thin edges of sectioned bone and from PMMA entered into the collected data as a result of the intention to indent across regions of bone tissue by starting and ending in the surrounding PMMA. These data were not representative of bone tissue properties, and were removed from the dataset by inspection and filtering. Inspection of the load-displacement curves revealed that the loading segments were not smooth for indentations that were near or at a PMMA-bone edge. These indent locations were verified using the objective in the nanoindenter, then deleted from the dataset. There were low modulus measurements that remained in the dataset, the majority of which were from indentations that were made in PMMA regions surrounding trabeculae and near the edges of trabeculae, with a minority of measurements that were made within osteocyte lacunae and within cracks. These low modulus measurements had values close to the modulus of the surrounding PMMA, thus we removed them on grounds that they were mechanically indistinguishable from PMMA. A filter threshold was chosen to segregate remaining indents of low and high modulus. The bimodal distribution of modulus data indicates a clear separation between high modulus values and low modulus values (Fig. 3a). The valley between peaks was chosen as the threshold. Data with moduli of less than 8 GPa were excluded from the analyses of bone mechanical properties. The distributions of trabecular modulus values for each group had shapes similar to that of all indents pooled (**Fig 3a**). The majority of the low modulus measurements were from the indents positioned at the ends of each linear array test for trabecular bone, resulting from our method of intentionally positioning the ends of the arrays in the surrounding PMMA. The contact hardness values corresponding to the excluded moduli were also excluded from analysis of the contact hardness data. Cortical bone data below 8 GPa were also discarded from the analysis (Fig. 3b).

Quantitative backscattered electron microscopy (qBSE)

Gray-scale levels in backscattered images of bone correlate with atomic number and mineral content [30, 31]. The bone specimen blocks were scanned at 300× magnification (Fig. 4) using a scanning electron microscope (FEI XL 30, FEI, Hillsboro, OR) equipped with a solid-state backscatter detector (FEI, model PW6843/00) at 30-kV excitation voltage and 15 mm working distance. To make the surfaces electrically conductive, each biopsy block was sputter coated with carbon (Edwards 306 Vacuum Coating System, Edwards Ltd., United Kingdom) to approximately 250 Angstroms thickness. For each specimen, five different trabeculae, irrespective of orientation, were selected at random to be imaged. Three cortical regions were also imaged. Regions selected for imaging were not necessarily the same as the regions that were tested by nanoindentation. Degrees of mineralization were assessed from

NIH-PA Author Manuscript

NIH-PA Author Manuscript

NIH-PA Author Manuscript

the images by converting bone gray-scale pixel values to atomic number (Z) using a calibration relationship based on standard materials of known average Z: aluminum (Z=13), magnesium oxide (Z=10.412), silicon dioxide (Z=10.805), and calcium carbonate (Z=12.57). Images of the calibration standard materials were taken before and after collecting each bone specimen to account for fluctuations in the system electronics. A calibration relationship was constructed by fitting a least squares regression between the gray-scale level measurements and the mean atomic numbers of the standards. Pixel resolution of the images was 0.278 μm. All images were collected by a single operator.

Images were analyzed for mean and standard deviation of mineral density using ImageJ (National Institutes of Health, Bethesda, MD). Area-weighted mean and standard deviation of mineralization density for each biopsy were calculated from the five trabecular images and three cortical images. Bone pixel gray-scale values were pooled into two histograms for each biopsy specimen (cortical and trabecular). Mean and standard deviation of mineral density were calculated from each histogram of the pooled pixel gray-scale values.

Statistical Analysis

Mean and standard deviation of elastic modulus, contact hardness, resistance to plastic deformation, and mineral density measurements were calculated for both trabecular and cortical regions of each biopsy. The effects of treatment groups (YgN, AMN, OP, and SSBT) on elastic modulus, contact hardness, and plastic deformation resistance were modeled using nested ANOVAs with sub-sampling. Each ANOVA was a mixed-effects model in which group was a fixed effect and the individual was a random effect. Variance component estimates were made using the restricted maximum likelihood analysis to characterize within and between individual variability. To compare the within-individual variability in the mechanical properties among groups, the standard deviations of the set of indentation measurements for each individual were compared by group using a one-way fixed-effect ANOVA. The effect of group on mineralization density was also analyzed using a fixed-effect, one-way ANOVA. Significant pair-wise comparisons were identified using Tukey's Honest Significant Difference multiple comparisons test. Simple linear regression was used to determine if correlations existed between the bone formation rates, mechanical properties and mineral density when biopsies were pooled. Differences in modulus-plastic deformation resistance relationships by bone region (trabecular/cortical) were assessed using multiple linear regression. Mechanical property measurements were averaged by biopsy for the regression analyses. Analysis of cortical bone data included 54 biopsies, since one biopsy from the osteoporotic group did not have a cortical bone region exposed to the block surface. All analyses were conducted using JMP 9.0 (SAS Institute Inc., Cary, NC). Statistical significance was defined as $p<0.05$.

Group differences in mechanical properties were initially analyzed for the HFH biopsies only (N=50), since embedding and sample preparation of those biopsies were performed by a uniform protocol. When all 55 biopsies were analyzed, laboratory (HFH or SMC) was included as a nominal covariate, since elastic modulus of the embedding material (PMMA) varied among the biopsies. PMMA modulus of the HFH samples (4.15 (0.24) GPa) was more than twice as large as that of the SMC samples (2.02 (0.44) GPa). Although the SSBT biopsies from the HFH had higher modulus than the SMC biopsies, the contact hardness did not differ between the laboratories

NIH-PA Author Manuscript

NIH-PA Author Manuscript

NIH-PA Author Manuscript

Results

Mechanical properties

Trabecular bone contact hardnesses, elastic moduli, and plastic deformation resistances of HFH biopsies were different among the groups ($p<0.001$, $p<0.001$, $p=0.002$, respectively; Table 2). SSBT trabecular bone tissue had higher contact hardness and higher plastic deformation resistance than the three comparison groups, while the comparison groups were not different from each other for either property. Trabecular bone elastic modulus from the SSBT group was higher than the moduli of the young normal group and of the osteoporotic group. The young normal group and the osteoporotic group did not have different trabecular elastic moduli. Trabecular elastic modulus of the age-matched normal group was not different from the other three groups. Cortical bone plastic deformation resistance was significantly different among the groups, with the SSBT group having greater resistance to plastic deformation than age-matched normal and osteoporotic groups ($p=0.01$, Table 2). Age-matched normal and osteoporotic groups did not have different cortical plastic deformation resistances, and the young normal group did not have different plastic deformation resistance compared to the other three groups. Cortical bone moduli and contact hardnesses were not different among the groups.

Group differences and pair-wise differences in trabecular bone contact hardness, modulus, and plastic deformation resistance did not change when both HFH and SMC biopsies were included in the analysis ($p<0.001$, $p=0.002$, $p<0.001$, respectively; Table 2, Fig. 5). The laboratory covariate was significant in the modulus model ($p=0.003$) but not in the contact hardness or plastic deformation resistance models ($p=0.34$, $p=0.69$). Cortical bone plastic deformation resistance was again different among groups ($p=0.003$), with the SSBT group having higher resistance to plastic deformation than all three comparison groups. Cortical moduli and contact hardnesses were still not different among groups. When cortical and trabecular data were analyzed together, plastic deformation resistance was lower in cortical bone compared to trabecular bone in the age-matched normal, osteoporotic, and SSBT groups. The plastic deformation resistance was not different between cortical and trabecular regions for the young normal group. The results from the analyses of mechanical properties were not sensitive to the threshold value used to filter the data, because results were similar when threshold values of 2, 4, and 6 GPa were used instead of 8 GPa in those analyses.

The multiple measurements taken of each biopsy allowed for the analysis of the variability in properties. The variance in the mechanical property data was mostly due to within-individual variation (84–87%) and less due to among-individual variation (13 to 16%). Within-individual variabilities in trabecular contact hardness and trabecular plastic deformation resistance were significantly different among the four groups ($p=0.012$, $p=0.015$; Fig. 6a, e). Young normal trabecular bone had significantly greater standard deviation in contact hardness than that of osteoporotic patients. SSBT trabecular bone had plastic deformation properties that were more variable than those of age-matched normal and osteoporotic groups. Standard deviations of elastic moduli and plastic deformation resistances of cortical bone were different among groups ($p=0.011$, $p=0.003$; **Fig 6d, f**). The SSBT group had more variable plastic deformation cortical bone properties than older normal and osteoporotic groups. In contrast, the SSBT group had less variable cortical bone modulus than the age-matched and young normal groups. Standard deviations in trabecular modulus and cortical contact hardness were not significantly different among the groups.

Mineral densities

Trabecular bone mean mineral densities were significantly different among the four groups ($p=0.018$, Fig. 7). No two groups had significantly different mineral densities by Tukey's

NIH-PA Author Manuscript

NIH-PA Author Manuscript

NIH-PA Author Manuscript

post-hoc analysis. However, there was a trend of higher mineral density in the trabecular bone of the SSBT group compared to the age-matched normal and osteoporotic groups (p=0.059 and 0.062, respectively). Variability in trabecular bone mineral densities were not different among the groups (p=0.077). Mean and standard deviation of cortical bone mineral densities were not different among the four groups. One SSBT biopsy exhibited substantial charging when imaged in the electron microscope and was excluded from the mineral density analysis.

Regression analyses

BFR was significantly, but weakly, associated with trabecular contact hardness, where contact hardness decreased with increasing BFR (p=0.006, r^2_{adj}=0.12, Fig. 8a). Similarly, BFR was weakly associated with trabecular plastic deformation resistance (p=0.007, r^2_{adj}=0.11, Fig. 8c). BFR and trabecular bone elastic modulus were not significantly associated, however the data indicated a weak trend of decreasing elastic modulus with increasing BFR (p=0.08, r^2_{adj} =0.04, Fig. 8b). BFR was not significantly associated with cortical bone modulus, contact hardness, or plastic deformation resistance. Furthermore, BFR was not significantly associated with mineral density of cortical or trabecular bone. When one influential sample was omitted, there was a significant, weak, trend for high mineral densities in trabecular bone in samples with low BFR (p=0.038, r^2_{adj}=0.06, **Fig 8d)**. The omitted biopsy was from an osteoporotic patient with unusually high bone formation rate (67.1 $\mu m^3/\mu m^2/yr$).

Mineral density was not significantly correlated with average elastic modulus, contact hardness, or resistance to plastic deformation.

Elastic modulus was weakly associated with plastic deformation resistance for both trabecular and cortical bone regions (p=0.046, r^2_{adj} = 0.06, and p=0.034, r^2_{adj} = 0.07, respectively; **Fig 9a, b**). Cortical and trabecular bone regions had different modulus-plastic deformation resistance relationships. On average, cortical bone modulus was significantly higher than trabecular bone modulus for a given plastic deformation resistance value; however, the slopes of these relationships were not different depending on bone region.

Discussion

The results support our hypothesis that tissue level properties, as measured by nanomechanical properties and tissue mineral density, are different for iliac bone biopsies from long-term bisphosphonate treated SSBT patients with atypical femoral fractures compared to those from age-matched and young normals, as well as from age-matched osteoporotic patients with vertebral fractures. Interestingly, both cortical and trabecular bone plastic deformation resistance were higher in the SSBT group than in the comparison groups. The magnitudes of the differences in plastic deformation resistance ranged from 15 to 22% in cortical bone and 29 to 31% in trabecular bone. SSBT trabecular bone also had higher modulus and exhibited a trend toward higher mineral content than the comparison groups, though the differences in mineral content among the groups were modest (1.7 to 2.4%). The average BFR of the SSBT group was close to zero; in contrast, among the age-matched groups, BFR was 54 fold greater in the osteoporotic group and 48 fold greater in the normal group, compared to the SSBT group. We suggest that differences in SSBT trabecular bone quality are consistent with increased tissue age due to the low BFR of these patients. However the higher resistance to plastic deformation, particularly in cortical bone, may indicate a possible connection between hard tissue plastic deformation properties and toughness properties. Cortical bone mean elastic properties were not different among the groups.

NIH-PA Author Manuscript

NIH-PA Author Manuscript

NIH-PA Author Manuscript

The average mechanical properties and mineral densities of trabecular and cortical bone were not different among the young normal, age-matched normal, and osteoporotic groups. This indicates that the average iliac bone material properties were not detectably altered by age or osteoporosis in our study. In contrast, SSBT cortical bone had higher plastic deformation resistance, and SSBT trabecular bone had higher contact hardness modulus, plastic deformation resistance, and a trend toward higher mineral density, compared to that of osteoporotics. We suggest that SSBT bone quality is different from bisphosphonate-naïve osteoporotics, but the differences cannot be directly attributed to bisphosphonate treatment, SSBT, or the combination of these effects, due to the study design.

Plastic deformation resistance was greater in trabecular bone regions compared to cortical bone regions, except in younger normal subjects. Aging may affect the ability for cortical bone to resist plastic deformation at the material level, relative to trabecular bone. However SSBT bone had greater plastic deformation resistance in both trabecular and cortical regions compared to the other groups. A combination of aging effects, disease and drug interactions may contribute to the ability for bone material to absorb energy through permanent deformation.

Heterogeneity in mechanical properties and mineral densities at the micrometer scale may be beneficial to the mechanical integrity of bone tissue by preventing propagation of cracks [32–36]. The relatively low variation in SSBT cortical bone elastic modulus compared to the normal groups is consistent with this hypothesis, as SSBT fractures occurred in regions composed primarily of cortical bone. This finding is also consistent with studies that have shown that bisphosphonate treatment is associated with decreased heterogeneity in the spectroscopic markers mineral/matrix ratio, crystallinity, carbonate/amide I ratio [37, 38], and mineral density distribution [39, 40]. Additionally, the trabecular bone of the osteoporotic group had less variable contact hardness properties, and a trend of less variable mineral densities (not shown), than that of the young normal group. A lack of heterogeneity in the cortical hard tissue of SSBT patients and trabecular hard tissue of osteoporotic patients may be associated with atypical and vertebral fractures, respectively, due to decreased resistance to crack propagation. However, the heterogeneity hypothesis was not supported by the plastic deformation resistance variability data. The standard deviation of plastic deformation resistance was high in the SSBT group for both cortical and trabecular bone. One possible explanation is that the positive effect of variability in properties has less impact when the properties are high on average. The mean plastic deformation resistance was higher in SSBT; therefore any beneficial effect of the heterogeneity in properties could be obviated. We did not measure fracture toughness directly nor measure cracking, thus we do not have data to relate cracking or toughness with plastic deformation resistance.

Studies with bisphosphonate-treated dogs have demonstrated changes in trabecular bone properties associated with drug treatment; however the data for cortical bone property changes with bisphosphonate treatment is less clear. In a recent study [41], dogs were treated for as many as three years with alendronate at one of two dosage levels: 0.2 mg/kg/day, which approximates treatment for postmenopausal osteoporosis on a milligram per kilogram basis, or five times the clinical dose at 1.0 mg/kg/day. Cortical bone mechanical properties were not different between alendronate-treated and vehicle-treated animals as measured by four-point bending of femur specimens. However beagle dogs treated with high dose alendronate were found to have lower toughness in rib cortical bone [42], indicating that the drug effect on cortical bone properties may be site specific, or evident only at high doses. High dose alendronate treatment was associated with lower toughness and increased strength in the trabecular bone of the vertebrae [12]. Changes in trabecular bone were also found at the postmenopausal osteoporosis treatment dose, such as increased microdamage [43], decreased toughness [44] and increased indentation contact hardness [45].

NIH-PA Author Manuscript

NIH-PA Author Manuscript

NIH-PA Author Manuscript

The associations of mechanical properties with bone formation rate in this study are consistent with our previous work [46] and consistent with the change in mechanical properties of bone tissue with increasing tissue age [47]. Trabecular contact hardness and plastic deformation resistance both increased with decreasing BFR, and trabecular modulus exhibited a trend of higher modulus in low BFR subjects. Trabecular mineral density increased with decreasing BFR, indicating that changes in mechanical properties may correspond with changes in mineral composition. These results are consistent with previous work in which mechanical properties of iliac biopsies from high and low bone turnover subjects were measured [46]. Low bone turnover was associated with high contact hardness and modulus in trabecular tissue within both the normal subject group and the vertebral fracture group, while no differences in mechanical properties were observed based on fracture status (fracture/non-fracture). We note that in the present study the BFR effect explained only 12%, 4%, 11%, and 6% of the variability in contact hardness, modulus, plastic deformation resistance, and mineral density, respectively, indicating that there was substantial variability due to effects other than BFR.

Elastic modulus and plastic deformation resistance were only weakly correlated. A study of nanoindentation properties in trabecular bone reported no significant relationship between modulus and plastic deformation resistance [48]. The weak relationship between plastic deformation resistance and elastic modulus is interesting because it indicates that the two properties may characterize different aspects of the bone hard tissue and provide independent information about the tissue. Trabecular and cortical bone modulus versus plastic deformation resistance relationships were significantly different from each other, with similar slopes but different intercepts. This indicated that for a given plastic deformation resistance value, the predicted modulus was higher for cortical bone than for trabecular bone but that the change in modulus per change in plastic deformation resistance was not different by bone region.

The experimental design was complicated by the fact that our sample set consisted of biopsies from two laboratories, in which biopsies were prepared and embedded by laboratory-specific protocols. The laboratory effect factored significantly in highlighting group differences in trabecular modulus ($p=0.002$ and $p=0.053$ with and without laboratory effect, respectively). In the analyses for trabecular and cortical plastic deformation resistance and trabecular contact hardness, the laboratory effect was not significant. In those models, the magnitudes of the group differences were large and likely masked any effect due to the laboratory. It is possible that the laboratory effect was associated with the difference in embedding PMMA properties between laboratories, in which the embedding PMMA for SMC biopsies was less than half as stiff as that used for HFH biopsies. However, the laboratory effect may be a confounding variable for other unmeasured parameters that account for some variability in the elastic modulus data. We suggest that embedding material modulus may be important to monitor when studying a biopsy collection from multiple laboratories or a set of biopsies prepared by multiple embedding protocols, though this effect may be confounded by parameters that were not accounted for in the study design.

We note that interpretation of our results is limited by a cohort effect, since the age-matched normal biopsies, young normal biopsies, and osteoporotic fracture biopsies were collected before 1992, while SSBT biopsies were collected within the last decade. Though two of the three comparison groups were age-matched to the SSBT group, the results may have been influenced by the different birth cohorts. Therefore, generalizations of the current observations should be made with caution.

NIH-PA Author Manuscript

NIH-PA Author Manuscript

NIH-PA Author Manuscript

Another limitation is the variability in the age of the biopsies, from the time of biopsy collection to the time when measurements were made for this study. Storage of biopsies can influence the nanoindenter-measured mechanical properties of embedded bone tissue [49]. Mittra and colleagues compared the mechanical property measurements of canine cancellous bone embedded in four different epoxies. Elastic modulus of bone was found to increase significantly when measured six months after the tissue was embedded compared to the modulus measured immediately after embedding, while contact hardness did not change over time. While extrapolation of these results to the present study is limited due to the relatively short storage time window monitored, and the fact that PMMA was not one of the materials examined in this study, we note mechanical property differences found in our present study exhibit an opposite trend to the storage time effect. The biopsies from normal subjects and osteoporotic patients in our study had been stored for as long as thirty years, however the SSBT biopsies were stored for less than ten years and had stiffer and harder properties than the biopsies from other groups. Therefore we expect that the mechanical property differences detected in our study to be robust even with the variability in time from embedding to nanoindentation testing.

Regardless of the limitations of the study, differences between SSBT patients and control subjects indicate that fractures at cortical bone sites were associated with differences in tissue properties at a distant site. Plastic deformation resistance was higher in SSBT cortical and trabecular bone, indicating that changes in the plastic behavior of bone tissue may be associated with SSBT and/or long-term bisphosphonate treatment. The differences in mechanical and mineralization properties of trabecular tissue were consistent with trends associated with tissue aging, though these properties were only partially and weakly explained by BFR. Interestingly, cortical bone plastic deformation resistance properties were different in SSBT and not the elastic properties. The collagen component of bone tissue is associated with the post-yield properties of bone [50, 51], thus future studies may elucidate whether bone quality measures of the organic component, such as crosslinks, can help to explain the SSBT fractures.

Obviously, these associations are statistical rather than causal and must be interpreted cautiously. It is well known that the iliac bone biopsy is a useful but not a perfect model for bone remodeling and mechanical property differences at other sites of the skeleton. Consequently, direct examination of bone mechanical properties at the sites of fractures associated with SSBT will be necessary to make strong conclusions. In addition, comparison of the nanomechanical properties of bisphosphonate-treated patients with and without atypical fractures and/or SSBT must be performed before attributing any causal role for the nanomechanical differences we observed in the current study.

Conclusion

Iliac bone biopsy samples from patients with severely suppressed bone turnover (SSBT), as identified clinically by Odvina and coauthors [14, 15], had higher cortical and trabecular plastic deformation resistance than those from the untreated osteoporotic group, young normal group, and age-matched normal group. The SSBT group also had higher contact hardness than the three comparison groups, higher tissue modulus than the untreated osteoporotic group and the young normal group, and slightly higher trabecular mineral density than the age-matched normal group and osteoporotic group. While differences in trabecular bone properties were consistent with the differences in bone formation rate, the higher plastic deformation resistance in SSBT cortical bone indicated that changed plastic deformation properties might be associated with atypical fractures. Additionally, SSBT cortical bone modulus was less heterogeneous than that of the normal groups, which may be associated with decreased resistance to crack propagation. We tentatively conclude that

NIH-PA Author Manuscript

NIH-PA Author Manuscript

NIH-PA Author Manuscript

SSBT and/or long-term bisphosphonate treatment may be associated with high plastic deformation resistance properties and less heterogeneous elastic properties of the hard tissue, in addition to extremely low bone formation rate.

Acknowledgments

We wish to thank Dr. Julie Schoenung and Dr. Enrique Lavernia for providing essential equipment, training and advice for the nanoindentation measurement system; Dr. Sarah Roeske for providing training and access to the carbon coating equipment; Patricia Kysar for training and advice on the SEM; Dr. Joseph Zerwekh of SMC for histomorphometric measurements and helpful discussions; Dr. Shijing Qiu of HFH for helpful discussions; Ms. Saroj Palnitkar for bone histomorphometric measurements at the HFH; Tyler Franklin for processing SEM images. This study is supported by National Institutes of Health (NIH) grant AR040776 (DPF). Statistical support was made possible by grant UL1 RR024146 from the National Center for Research Resources (NCRR), a component of the NIH, and NIH Roadmap for Medical Research. Its contents are solely the responsibility of the authors and do not necessarily represent the official view of NCRR or NIH.

Abbreviations

SSBT	severely suppressed bone turnover
E	elastic modulus
H_c	contact hardness
H	plastic deformation resistance
BFR	bone formation rate
Z	atomic number
PMMA	poly(methyl methacrylate)

References

[1]. Kanis JA, Melton LJ 3rd, Christiansen C, Johnston CC, Khaltaev N. The diagnosis of osteoporosis. J Bone Miner Res. 1994; 9:1137–41. [PubMed: 7976495]

[2]. Abrahamsen B, Eiken P, Eastell R. Cumulative Alendronate Dose and the Long-Term Absolute Risk of Subtrochanteric and Diaphyseal Femur Fractures: A Register-Based National Cohort Analysis. J Clin Endocrinol Metab.

[3]. Black DM, Kelly MP, Genant HK, Palermo L, Eastell R, Bucci-Rechtweg C, Cauley J, Leung PC, Boonen S, Santora A, de Papp A, Bauer DC. Bisphosphonates and Fractures of the Subtrochanteric or Diaphyseal Femur. N Engl J Med. 2010

[4]. Girgis CM, Sher D, Seibel MJ. Atypical femoral fractures and bisphosphonate use. N Engl J Med. 2010; 362:1848–9. [PubMed: 20463351]

[5]. Lenart BA, Lorich DG, Lane JM. Atypical fractures of the femoral diaphysis in postmenopausal women taking alendronate. N Engl J Med. 2008; 358:1304–6. [PubMed: 18354114]

[6]. Lenart BA, Neviaser AS, Lyman S, Chang CC, Edobor-Osula F, Steele B, van der Meulen MC, Lorich DG, Lane JM. Association of low-energy femoral fractures with prolonged bisphosphonate use: a case control study. Osteoporos Int. 2009; 20:1353–62. [PubMed: 19066707]

[7]. Park-Wyllie LY, Mamdani MM, Juurlink DN, Hawker GA, Gunraj N, Austin PC, Whelan DB, Weiler PJ, Laupacis A. Bisphosphonate use and the risk of subtrochanteric or femoral shaft fractures in older women. JAMA. 2011; 305:783–9. [PubMed: 21343577]

[8]. Shane E, Burr D, Ebeling PR, Abrahamsen B, Adler RA, Brown TD, Cheung AM, Cosman F, Curtis JR, Dell R, Dempster D, Einhorn TA, Genant HK, Geusens P, Klaushofer K, Koval K, Lane JM, McKiernan F, McKinney R, Ng A, Nieves J, O'Keefe R, Papapoulos S, Sen HT, van der Meulen MC, Weinstein RS, Whyte M. Atypical subtrochanteric and diaphyseal femoral fractures: Report of a task force of the American Society for Bone and Mineral Research. J Bone Miner Res.

NIH-PA Author Manuscript

NIH-PA Author Manuscript

NIH-PA Author Manuscript

[9]. Burr DB, Forwood MR, Fyhrie DP, Martin RB, Schaffler MB, Turner CH. Bone microdamage and skeletal fragility in osteoporotic and stress fractures. J Bone Miner Res. 1997; 12:6–15. [PubMed: 9240720]

[10]. Komatsubara S, Mori S, Mashiba T, Li J, Nonaka K, Kaji Y, Akiyama T, Miyamoto K, Cao Y, Kawanishi J, Norimatsu H. Suppressed bone turnover by long-term bisphosphonate treatment accumulates microdamage but maintains intrinsic material properties in cortical bone of dog rib. J Bone Miner Res. 2004; 19:999–1005. [PubMed: 15125797]

[11]. Mashiba T, Hirano T, Turner CH, Forwood MR, Johnston CC, Burr DB. Suppressed bone turnover by bisphosphonates increases microdamage accumulation and reduces some biomechanical properties in dog rib. J Bone Miner Res. 2000; 15:613–20. [PubMed: 10780852]

[12]. Mashiba T, Turner CH, Hirano T, Forwood MR, Johnston CC, Burr DB. Effects of suppressed bone turnover by bisphosphonates on microdamage accumulation and biomechanical properties in clinically relevant skeletal sites in beagles. Bone. 2001; 28:524–31. [PubMed: 11344052]

[13]. Mashiba T, Mori S, Burr DB, Komatsubara S, Cao Y, Manabe T, Norimatsu H. The effects of suppressed bone remodeling by bisphosphonates on microdamage accumulation and degree of mineralization in the cortical bone of dog rib. J Bone Miner Metab. 2005; 23(Suppl):36–42. [PubMed: 15984412]

[14]. Odvina CV, Levy S, Rao S, Zerwekh JE, Sudhaker Rao D. Unusual mid-shaft fractures during long term bisphosphonate therapy. Clin Endocrinol (Oxf). 2010

[15]. Odvina CV, Zerwekh JE, Rao DS, Maalouf N, Gottschalk FA, Pak CY. Severely suppressed bone turnover: a potential complication of alendronate therapy. J Clin Endocrinol Metab. 2005; 90:1294–301. [PubMed: 15598694]

[16]. Stepan JJ, Burr DB, Pavo I, Sipos A, Michalska D, Li J, Fahrleitner-Pammer A, Petto H, Westmore M, Michalsky D, Sato M, Dobnig H. Low bone mineral density is associated with bone microdamage accumulation in postmenopausal women with osteoporosis. Bone. 2007; 41:378–85. [PubMed: 17597017]

[17]. Burr DB, Allen MR. Low bone turnover and microdamage? How and where to assess it? J Bone Miner Res. 2008; 23:1150–1. author reply 1152–3. [PubMed: 18348687]

[18]. Foldes J, Shih MS, Parfitt AM. Frequency distributions of tetracycline-based measurements: implications for the interpretation of bone formation indices in the absence of double-labeled surfaces. J Bone Miner Res. 1990; 5:1063–7. [PubMed: 2080717]

[19]. Parfitt AM, Drezner MK, Glorieux FH, Kanis JA, Malluche H, Meunier PJ, Ott SM, Recker RR. Bone histomorphometry: standardization of nomenclature, symbols, and units. Report of the ASBMR Histomorphometry Nomenclature Committee. J Bone Miner Res. 1987; 2:595–610. [PubMed: 3455637]

[20]. Oliver WC, Pharr GM. An Improved Technique for Determining Hardness and Elastic-Modulus Using Load and Displacement Sensing Indentation Experiments. Journal of Materials Research. 1992; 7:1564–1583.

[21]. Sakai M. The Meyer hardness: A measure for plasticity? Journal of Materials Research. 1999; 14:3630–3639.

[22]. Oyen ML. Nanoindentation hardness of mineralized tissues. J Biomech. 2006; 39:2699–702. [PubMed: 16253265]

[23]. Donnelly E, Baker SP, Boskey AL, van der Meulen MC. Effects of surface roughness and maximum load on the mechanical properties of cancellous bone measured by nanoindentation. J Biomed Mater Res A. 2006; 77:426–35. [PubMed: 16392128]

[24]. Hoffler CE, Guo XE, Zysset PK, Goldstein SA. An application of nanoindentation technique to measure bone tissue Lamellae properties. J Biomech Eng. 2005; 127:1046–53. [PubMed: 16502646]

[25]. Lucas BN, Oliver WC, Pharr GM, Loubet J-L. Time-Dependent Deformation During Indentation Testing. Mat. Res. Soc. Symp. Proc. 1996; 436

[26]. Zysset PK, Guo XE, Hoffler CE, Moore KE, Goldstein SA. Mechanical properties of human trabecular bone lamellae quantified by nanoindentation. Technol Health Care. 1998; 6:429–32. [PubMed: 10100945]

NIH-PA Author Manuscript

NIH-PA Author Manuscript

NIH-PA Author Manuscript

[27]. Kono R. The Dynamic Bulk Viscosity of Polystyrene and Polymethyl Methacrylate. Journal of the Physical Society of Japan. 1960; 15:718–725.

[28]. Ciarelli TE, Fyhrie DP, Parfitt AM. Effects of vertebral bone fragility and bone formation rate on the mineralization levels of cancellous bone from white females. Bone. 2003; 32:311–5. [PubMed: 12667559]

[29]. Hengsberger S, Kulik A, Zysset P. Nanoindentation discriminates the elastic properties of individual human bone lamellae under dry and physiological conditions. Bone. 2002; 30:178–184. [PubMed: 11792582]

[30]. Skedros JG, Bloebaum RD, Bachus KN, Boyce TM. The meaning of graylevels in backscattered electron images of bone. J Biomed Mater Res. 1993; 27:47–56. [PubMed: 8380598]

[31]. Skedros JG, Bloebaum RD, Bachus KN, Boyce TM, Constantz B. Influence of mineral content and composition on graylevels in backscattered electron images of bone. J Biomed Mater Res. 1993; 27:57–64. [PubMed: 8420999]

[32]. Fratzl P. Bone fracture: When the cracks begin to show. Nat Mater. 2008; 7:610–2. [PubMed: 18654582]

[33]. Fratzl P, Gupta HS, Fischer FD, Kolednik O. Hindered crack propagation in materials with periodically varying Young's modulus - Lessons from biological materials. Advanced Materials. 2007; 19:2657–+.

[34]. Gupta HS, Stachewicz U, Wagermaier W, Roschger P, Wagner HD, Fratzl P. Mechanical modulation at the lamellar level in osteonal bone. Journal of Materials Research. 2006; 21:1913–1921.

[35]. Peterlik H, Roschger P, Klaushofer K, Fratzl P. From brittle to ductile fracture of bone. Nat Mater. 2006; 5:52–5. [PubMed: 16341218]

[36]. Wang X, Zauel RR, Rao DS, Fyhrie DP. Cancellous bone lamellae strongly affect microcrack propagation and apparent mechanical properties: separation of patients with osteoporotic fracture from normal controls using a 2D nonlinear finite element method (biomechanical stereology). Bone. 2008; 42:1184–92. [PubMed: 18378204]

[37]. Boskey AL, Spevak L, Weinstein RS. Spectroscopic markers of bone quality in alendronate-treated postmenopausal women. Osteoporos Int. 2009; 20:793–800. [PubMed: 18769963]

[38]. Gourion-Arsiquaud S, Allen MR, Burr DB, Vashishth D, Tang SY, Boskey AL. Bisphosphonate treatment modifies canine bone mineral and matrix properties and their heterogeneity. Bone. 46:666–72. [PubMed: 19925895]

[39]. Roschger P, Rinnerthaler S, Yates J, Rodan GA, Fratzl P, Klaushofer K. Alendronate increases degree and uniformity of mineralization in cancellous bone and decreases the porosity in cortical bone of osteoporotic women. Bone. 2001; 29:185–91. [PubMed: 11502482]

[40]. Zoehrer R, Roschger P, Paschalis EP, Hofstaetter JG, Durchschlag E, Fratzl P, Phipps R, Klaushofer K. Effects of 3- and 5-year treatment with risedronate on bone mineralization density distribution in triple biopsies of the iliac crest in postmenopausal women. J Bone Miner Res. 2006; 21:1106–12. [PubMed: 16813531]

[41]. Burr DB, Diab T, Koivunemi A, Koivunemi M, Allen MR. Effects of 1 to 3 years' treatment with alendronate on mechanical properties of the femoral shaft in a canine model: implications for subtrochanteric femoral fracture risk. J Orthop Res. 2009; 27:1288–92. [PubMed: 19396816]

[42]. Allen MR, Reinwald S, Burr DB. Alendronate reduces bone toughness of ribs without significantly increasing microdamage accumulation in dogs following 3 years of daily treatment. Calcif Tissue Int. 2008; 82:354–60. [PubMed: 18463913]

[43]. Allen MR, Iwata K, Phipps R, Burr DB. Alterations in canine vertebral bone turnover, microdamage accumulation, and biomechanical properties following 1-year treatment with clinical treatment doses of risedronate or alendronate. Bone. 2006; 39:872–9. [PubMed: 16765660]

[44]. Allen MR, Burr DB. Three years of alendronate treatment results in similar levels of vertebral microdamage as after one year of treatment. J Bone Miner Res. 2007; 22:1759–65. [PubMed: 17663638]

NIH-PA Author Manuscript

NIH-PA Author Manuscript

NIH-PA Author Manuscript

[45]. Wang X, Allen MR, Burr DB, Lavernia EJ, Jeremic B, Fyhrie DP. Identification of material parameters based on Mohr-Coulomb failure criterion for bisphosphonate treated canine vertebral cancellous bone. Bone. 2008; 43:775–80. [PubMed: 18599390]

[46]. Wang X, Sudhaker Rao D, Ajdelsztajn L, Ciarelli TE, Lavernia EJ, Fyhrie DP. Human iliac crest cancellous bone elastic modulus and hardness differ with bone formation rate per bone surface but not by existence of prevalent vertebral fracture. J Biomed Mater Res B Appl Biomater. 2008; 85:68–77. [PubMed: 17696151]

[47]. Donnelly E, Boskey AL, Baker SP, van der Meulen MC. Effects of tissue age on bone tissue material composition and nanomechanical properties in the rat cortex. J Biomed Mater Res A. 2009

[48]. Smith LJ, Schirer JP, Fazzalari NL. The role of mineral content in determining the micromechanical properties of discrete trabecular bone remodeling packets. J Biomech. 2010

[49]. Mittra E, Akella S, Qin YX. The effects of embedding material, loading rate and magnitude, and penetration depth in nanoindentation of trabecular bone. J Biomed Mater Res A. 2006; 79:86–93. [PubMed: 16758456]

[50]. Jepsen KJ, Goldstein SA, Kuhn JL, Schaffler MB, Bonadio J. Type-I collagen mutation compromises the post-yield behavior of Mov13 long bone. J Orthop Res. 1996; 14:493–9. [PubMed: 8676263]

[51]. Zioupos P, Currey JD. Changes in the stiffness, strength, and toughness of human cortical bone with age. Bone. 1998; 22:57–66. [PubMed: 9437514]

NIH-PA Author Manuscript

NIH-PA Author Manuscript

NIH-PA Author Manuscript

Research Highlights

- Severely suppressed bone turnover (SSBT) patients had atypical fractures while on bisphosphonates.
- We measured tissue level mechanical properties and mineral density of iliac bone biopsies from SSBT, treatment-naïve osteoporotics, and normals.
- SSBT cortical and trabecular bone had greater plastic deformation resistance than controls.
- SSBT cortical bone had less heterogeneous elastic modulus properties than controls.
- Treatment-naïve osteoporotic bone properties were similar to those of young and age-matched normal bone.

NIH-PA Author Manuscript

NIH-PA Author Manuscript

NIH-PA Author Manuscript

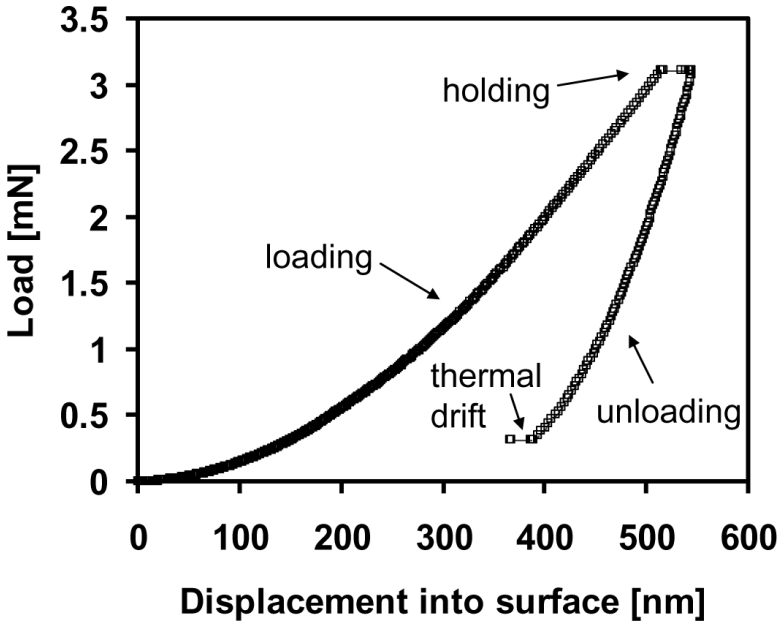

Fig. 1.

Representative nanoindentation load-displacement curve for 500 nm indent. Berkovich diamond tip loaded into the surface at a target strain rate of 0.05 s^{-1} to 500 nm depth. Tip was held at maximum load for 10 seconds, unloaded and held at 10% of maximum load for 100 seconds to calculate thermal drift. Elastic modulus and contact hardness were calculated from the unloading portion of the curve.

NIH-PA Author Manuscript

NIH-PA Author Manuscript

NIH-PA Author Manuscript

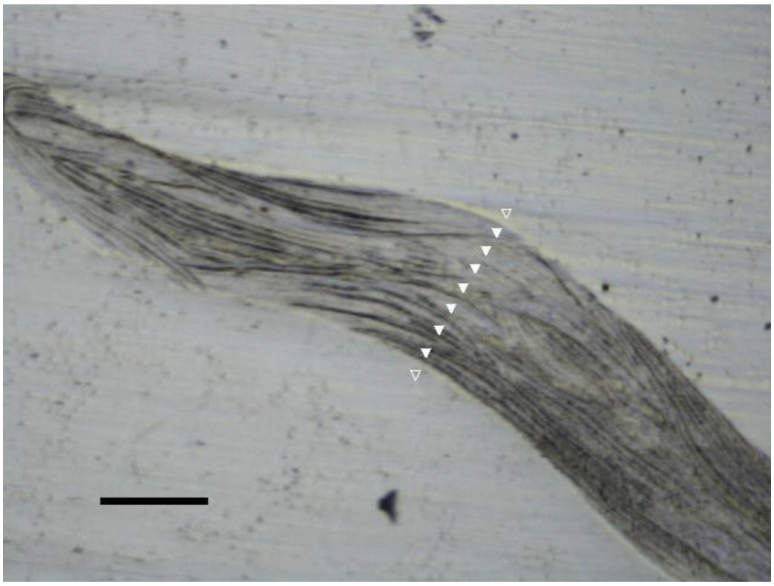

Fig. 2.

Image of a single trabecula from a biopsy imaged using the 10× objective in the nanoindenter. Example of a series of indentations shown in white triangles. Black scale bar represents 100 μm length. Indents in plastic regions (unfilled white triangles) were not included in the analysis. Spacing between indents was a minimum of 20 μm.

NIH-PA Author Manuscript

NIH-PA Author Manuscript

NIH-PA Author Manuscript

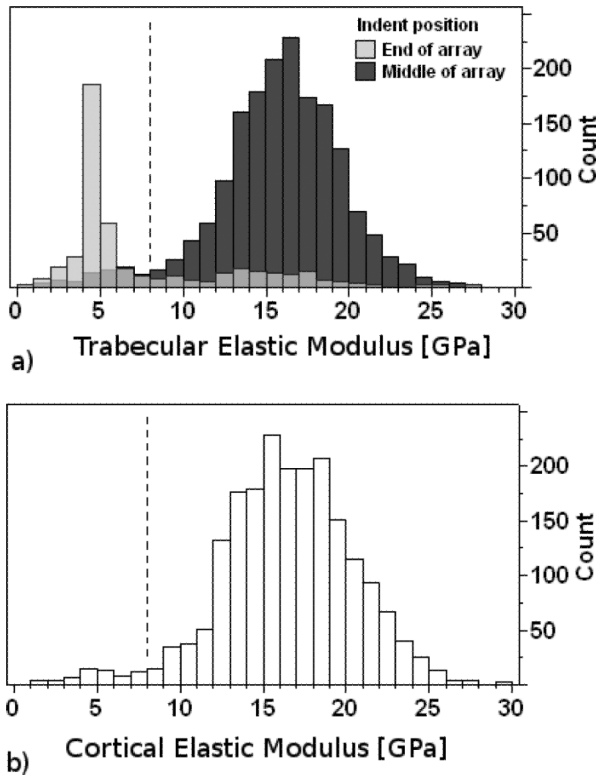

Fig. 3.

Histograms of elastic modulus values for all indents made in trabecular (a) and cortical (b) bone regions. Some mechanical property data from the thin edges of sectioned bone and from plastic entered into the data set as a result of the intention to indent across regions of bone tissue by starting and ending in the plastic region (Fig. 2). When the initial and final indents of each linear array were removed from the data set, the peak centered at the low modulus region (4 to 5 GPa) was greatly reduced (a; dark grey bars). In addition to indentations made in the plastic regions, other low modulus values were likely from indentations in lacunae and cracks (a; light grey bars). Low modulus values were indistinguishable from the modulus of the embedding material (4.15 and 2.02 GPa for HFH and SMC biopsies, respectively), thus these values were filtered out of the data set. Medium gray areas (a) show the overlapping regions of the 2 distributions. Data below 8 GPa (dotted black line) were eliminated from the analysis. Cortical bone indents below 8 GPa were not included in the analysis of cortical bone properties (b).

NIH-PA Author Manuscript

NIH-PA Author Manuscript

NIH-PA Author Manuscript

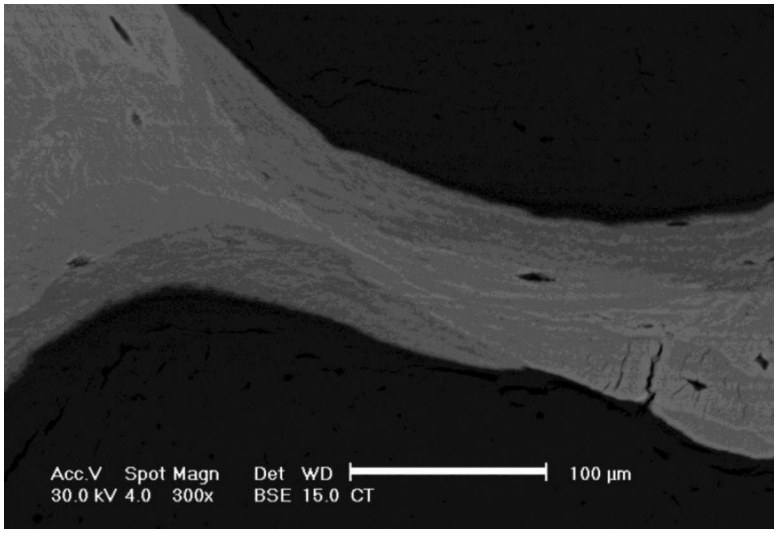

Fig. 4.

Backscattered electron microscope image of a trabecula of one biopsy. Grayscale levels correlate with the degree of mineralization. Lighter regions represent areas of higher mineral density than darker regions. Images were captured at 300×. Scale bar represents 100 μm.

NIH-PA Author Manuscript
NIH-PA Author Manuscript
NIH-PA Author Manuscript

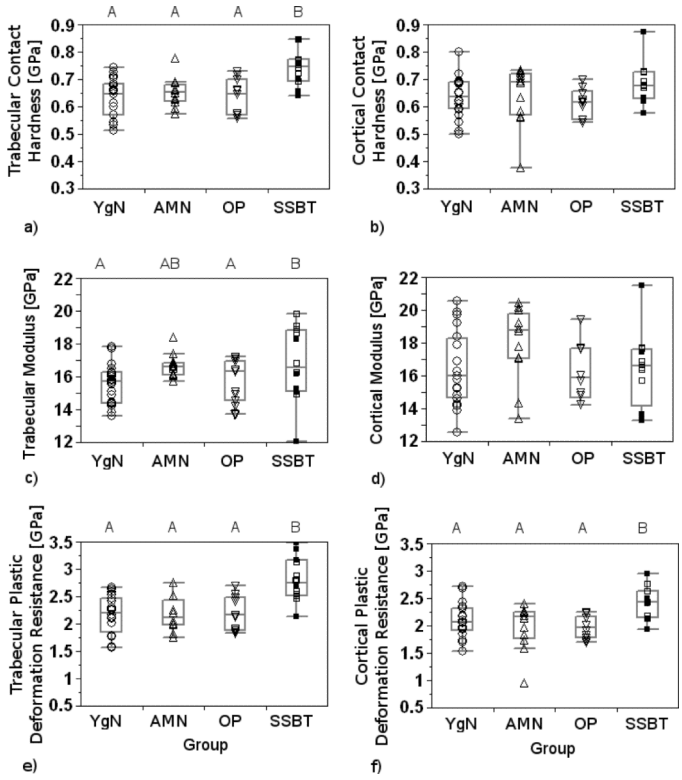

Fig. 5.

Box plots of contact hardnesses (a, b), elastic moduli (c, d), and plastic deformation resistances (e, f) of trabecular (a, c, e) and cortical bone (b, d, f) averaged by biopsy and reported by Group (YgN=Young Normals, AMN=Age-Matched Normals, OP=Osteoporotic, SSBT=Severely Suppressed Bone Turnover). Biopsies from Southwestern Medical Center (SMC) are represented by filled squares (■). All other biopsies were from Henry Ford Hospital (HFH). Groups with significantly different mechanical properties, when both SMC and HFH biopsies were included in the analysis, are denoted with different letters (Tukey post hoc tests). Significance level for all tests was $\alpha=0.05$.

NIH-PA Author Manuscript

NIH-PA Author Manuscript

NIH-PA Author Manuscript

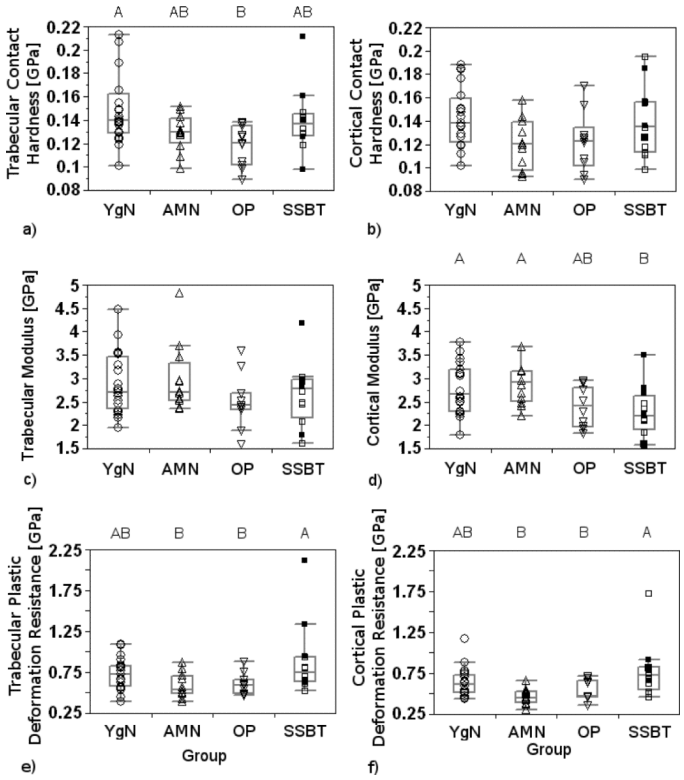

Fig. 6.

The average standard deviations of trabecular contact hardness (a), trabecular plastic deformation resistance (e), cortical modulus (d), and cortical plastic deformation (f) were significantly different among the four groups (ANOVA, p=0.012, p=0.015, p=0.011, p=0.003, respectively). Significance level for all tests was α=0.05. Groups with significantly different within-individual variability in properties are denoted with different letters (Tukey's HSD).

NIH-PA Author Manuscript

NIH-PA Author Manuscript

NIH-PA Author Manuscript

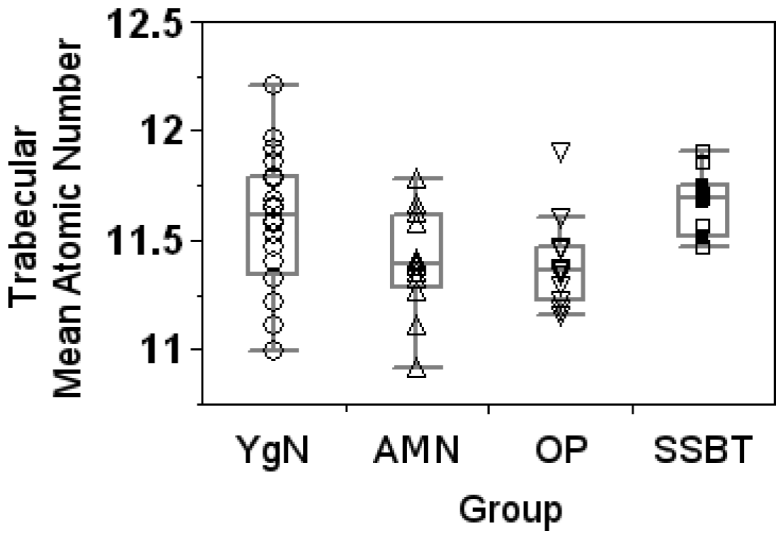

Fig. 7.

Mean mineral density of trabecular bone was significantly different among groups (ANOVA, p=0.018). There was a trend of higher mineral density in the trabecular bone of the SSBT group compared to the age-matched normal and osteoporotic groups (Tukey's HSD, p=0.059 and 0.062, respectively). Significance level for all tests was α=0.05.

NIH-PA Author Manuscript

NIH-PA Author Manuscript

NIH-PA Author Manuscript

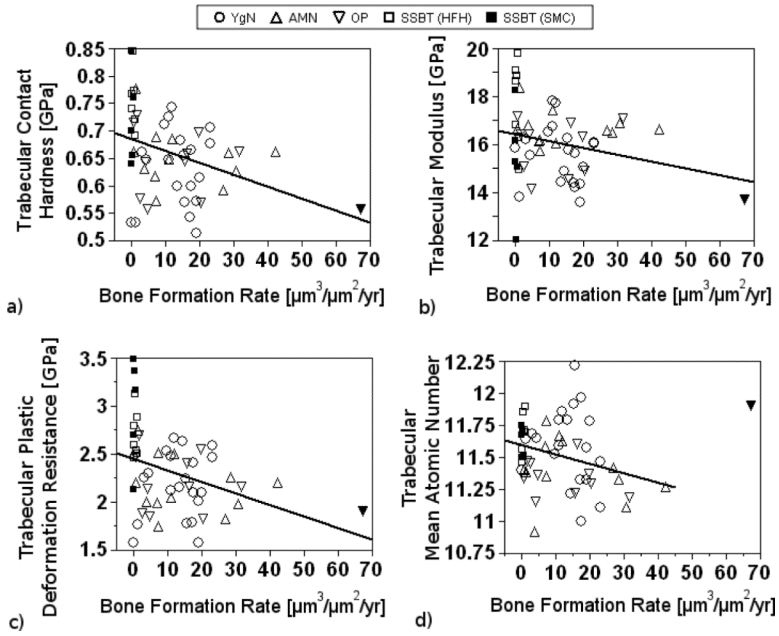

Fig. 8.

Trabecular contact hardness (a) and plastic deformation resistance (c) were each significantly but weakly correlated with BFR using simple linear regression ($p=0.006$, $r^2_{adj}=0.12$, and $p=0.007$, $r^2_{adj}=0.11$, respectively). Trabecular modulus and BFR (b) were not significantly associated but exhibited a trend for a weak association ($p=0.08$, $r^2_{adj}=0.04$). Trabecular mineral density and BFR (c) were significantly, but weakly, associated ($p=0.038$, $r^2_{adj}=0.06$) when one outlier (▼), an osteoporotic biopsy, was excluded from the analysis. The outlier was included in the analyses of the other regressions. Relationships between cortical bone tissue properties and BFR were not significant (not shown).

NIH-PA Author Manuscript

NIH-PA Author Manuscript

NIH-PA Author Manuscript

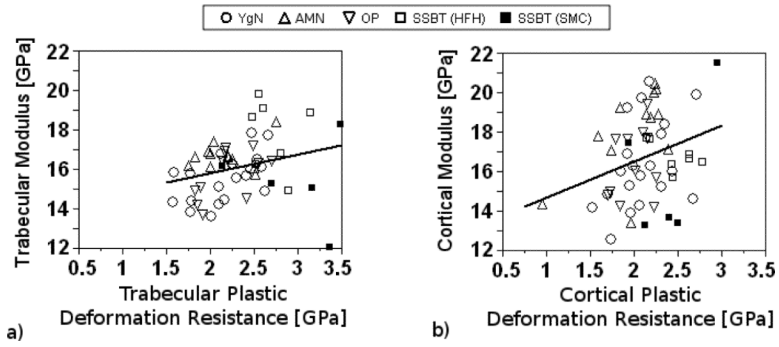

Fig. 9.

Regressions between modulus and plastic deformation resistance were significant but weak for trabecular (a) and cortical (b) regions ($p=0.046$, $r^2_{adj} = 0.06$, and $p=0.034$, $r^2_{adj} = 0.07$, respectively).

NIH-PA Author Manuscript NIH-PA Author Manuscript NIH-PA Author Manuscript

Table 1

Characteristics of study groups

Group	N	Laboratory	Osteoporotic	Bisphos- phonate	Fracture	Age- matched	Age (years) Range	Age (years) Mean (SD)	Trabecular bone formation rate (BFR)(μm³/μm²/year) Range	Trabecular bone formation rate (BFR)(μm³/μm²/year) Mean (SD)
Y gN	20	HFH	N	N	N	N	20–40	31.6[a] (5.6)	0–23.3	13.5[c] (6.9)
AMN	12	HFH	N	N	N	Y	49–74	63.8[b] (8.5)	0.6–42.3	14.8[c] (13.7)
OP	11	HFH	Y	N	lumbar vertebral	Y	53–76	65.5[b] (7.7)	0.5–67.1	16.7[c] (19.4)
SSBT	12	HFH (7), SMC (5)	Y	Y	atypical femur	Y	49–77	64.1[b] (9.3)	0–1.00	0.3[d] (0.4)

YgN - Young normal

AMN - Age-matched normal

OP - Osteoporotic

SSBT - Severely suppressed bone turnover

HFH - Henry Ford Hospital, Detroit, MI

SMC - Southwestern Medical Center, Dallas, TX

[a] values that do not share alphabetic superscripts within a column are statistically different ($p<0.05$)

[b] values that do not share alphabetic superscripts within a column are statistically different ($p<0.05$)

[c] values that do not share alphabetic superscripts within a column are statistically different ($p<0.05$)

[d] values that do not share alphabetic superscripts within a column are statistically different ($p<0.05$)

NIH-PA Author Manuscript NIH-PA Author Manuscript NIH-PA Author Manuscript

Table 2

Nanoindentation results summary

		Trabecular bone			Cortical bone		
Group	**N**	**E [GPa] ***	**H_c [GPa] †**	**H [GPa] §**	**E [GPa]**	**H_c [GPa]**	**H[GPa] §**
YgN	20	15.6 (1.2)^{a,1}	0.63 (0.07)^{a,1}	2.18 (0.34)^{a,1}	16.4 (2.2)^{a,1}	0.63 (0.075)^{a,1}	2.10 (0.3 l)$^{a\ b,1}$
AMN	12	16.7 (0.7)$^{a\ b,1\ 2}$	0.65 (0.05)^{a,1}	2.17 (0.30)^{a,1}	18.0 (2.2)^{a,1}	0.64 (0.1 l)^{a,1}	1.98 (0.41)^{a,1}
OP	11^	15.7 (1.3)^{a,1}	0.64 (0.06)^{a,1}	2.19 (0.31)^{a,1}	16.3 (1.8)^{a,1}	0.61 (0.052)^{a,1}	1.98 (0.21)^{a,1}
SSBT #	12						
HFH	7	17.8 (1.8)^{b};	0.76 (0.05)^{b};	2.71 (0.24)^{b}	16.8 (0.7)^{a};	0.70 (0.027)^{a};	2.46 (0.24)^{b}
HFH and SMC	12	16.8 (2.3)^{2}	0.74 (0.06)^{2}	2.82 (0.40)^{2}	16.4 (2.3)^{1}	0.69 (0.076)^{1}	2.42 (0.30)^{2}

Each cell reports mean value; standard deviation in parenthesis.

* E=elastic modulus

† H_C=contact hardness

§ H=plastic deformation resistance

^ N=10 for cortical bone measurements

\# top row values are from HFH biopsies only (n=7), bottom row values are from HFH and SMC biopsies, pooled (n=12)

a values that do not share alphabetic superscripts within a column are statistically different ($p<0.05$) for only HFH biopsies (n=50)

b values that do not share alphabetic superscripts within a column are statistically different ($p<0.05$) for only HFH biopsies (n=50)

1 values that do not share numeric superscripts within a column are statistically different ($p<0.05$) for HFH and SMC biopsies (n=55)

2 values that do not share numeric superscripts within a column are statistically different ($p<0.05$) for HFH and SMC biopsies (n=55)